

## Modelled three-dimensional suction accuracy predicts prey capture success in three species of centrarchid fishes

Emily A. Kane and Timothy E. Higham

*J. R. Soc. Interface* 2014 **11**, 20140223, published 9 April 2014

---

### Supplementary data

["Data Supplement"](#)

[http://rsif.royalsocietypublishing.org/content/suppl/2014/03/28/rsif.2014.0223.DC1.htm](http://rsif.royalsocietypublishing.org/content/suppl/2014/03/28/rsif.2014.0223.DC1.html)  
l

### References

[This article cites 55 articles, 22 of which can be accessed free](#)

<http://rsif.royalsocietypublishing.org/content/11/95/20140223.full.html#ref-list-1>

### Email alerting service

Receive free email alerts when new articles cite this article - sign up in the box at the top right-hand corner of the article or click [here](#)



## Research

**Cite this article:** Kane EA, Higham TE. 2014 Modelled three-dimensional suction accuracy predicts prey capture success in three species of centrarchid fishes. *J. R. Soc. Interface* **11**: 20140223.  
<http://dx.doi.org/10.1098/rsif.2014.0223>

Received: 3 March 2014

Accepted: 14 March 2014

### Subject Areas:

biomechanics

### Keywords:

ingested volume, capture success, suction accuracy, performance, prey capture

### Author for correspondence:

Emily A. Kane

e-mail: [ekane001@ucr.edu](mailto:ekane001@ucr.edu)

Electronic supplementary material is available at <http://dx.doi.org/10.1098/rsif.2014.0223> or via <http://rsif.royalsocietypublishing.org>.

# Modelled three-dimensional suction accuracy predicts prey capture success in three species of centrarchid fishes

Emily A. Kane and Timothy E. Higham

Department of Biology, University of California, 900 University Avenue, Riverside, CA 92521, USA

Prey capture is critical for survival, and differences in correctly positioning and timing a strike (accuracy) are likely related to variation in capture success. However, an ability to quantify accuracy under natural conditions, particularly for fishes, is lacking. We developed a predictive model of suction hydrodynamics and applied it to natural behaviours using three-dimensional kinematics of three centrarchid fishes capturing evasive and non-evasive prey. A spheroid ingested volume of water (IVW) with dimensions predicted by peak gape and ram speed was verified with known hydrodynamics for two species. Differences in capture success occurred primarily with evasive prey (64–96% success). *Micropterus salmoides* had the greatest ram and gape when capturing evasive prey, resulting in the largest and most elongate IVW. Accuracy predicted capture success, although other factors may also be important. The lower accuracy previously observed in *M. salmoides* was not replicated, but this is likely due to more natural conditions in our study. Additionally, we discuss the role of modulation and integrated behaviours in shaping the IVW and determining accuracy. With our model, accuracy is a more accessible performance measure for suction-feeding fishes, which can be used to explore macroevolutionary patterns of prey capture evolution.

## 1. Introduction

The ability to capture prey is critical for survival in predatory animals. Capture strategies vary depending on specializations in predator and prey, and the outcome is determined by performance and behaviour of both the predator and prey [1–5]. For predators, a large component of success is likely due to strike accuracy, or the ability to correctly position and time a strike [6]. In this way, accuracy is the link between feeding performance (how well predators perform feeding behaviours) and predator success (whether or not prey are captured), and acts as an ecologically relevant measure of capture performance [7]. However, despite the importance of accuracy to predator strategies, our understanding of the determinants of predator success is poor, particularly in suction-feeding fishes (but see [6,8–10]).

Suction is a widespread predatory strategy used by fishes [11–14], and accuracy is particularly important for these predators, but quantifying accuracy has been difficult. Suction is generated by rapidly expanding the mouth cavity, creating a pressure gradient that draws water and prey into the mouth [14–19]. Because suction force decays rapidly with distance from the mouth [17,20], predators must accurately position and time the suction field to successfully entrain prey [19,20]. The term ‘accuracy’ has been used synonymously with capture success, where predators with greater success are assumed to be more accurate [21–26]. However, a successful prey capture event depends on several factors related to both the predator and prey [8], and accuracy may not be directly related to success. Another more direct method linearly relates predator and prey position [6,19,27]. However, it may not be relevant for suction-feeding fishes, where predators rely on a volume of water positioned anterior to their jaws to capture prey [17,18,20,28,29], rather than their jaws directly. Therefore, predator accuracy should instead be quantified relative to the ingested volume of water (IVW) [28,29]. This requires fluid visualization techniques such as digital particle

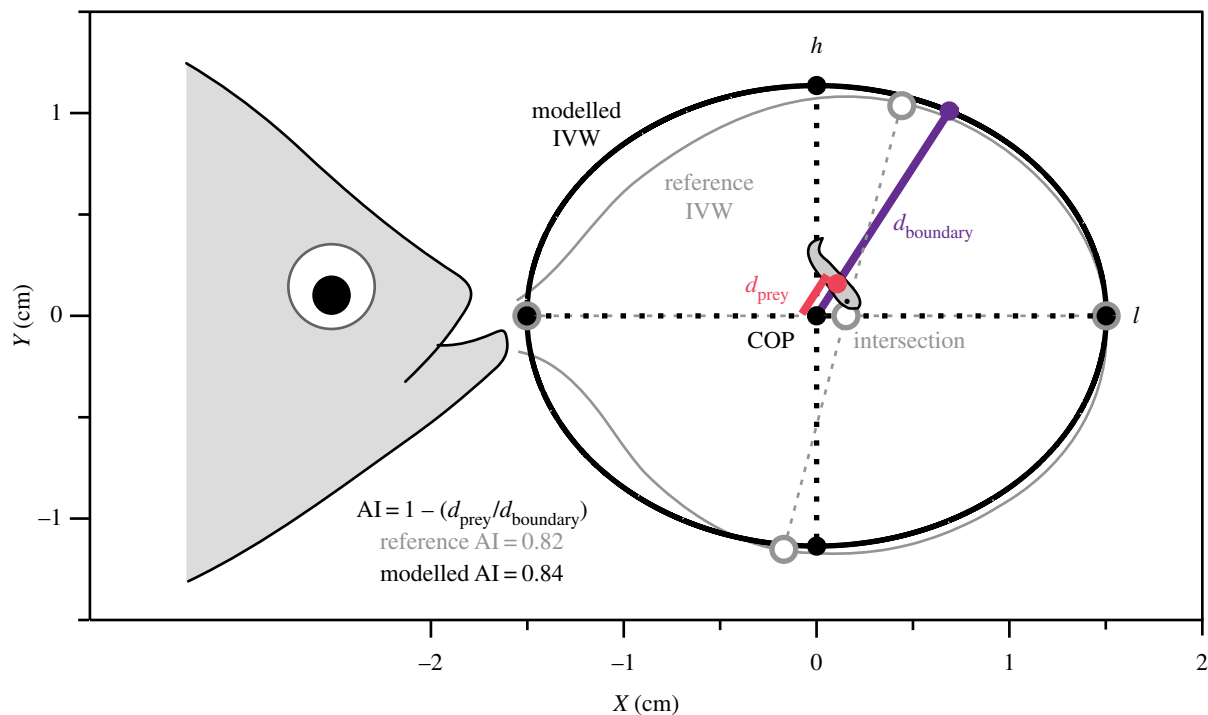


**Figure 1.** Comparison of reference and modelled IVW shapes. Open grey circles show the top, left, bottom and right boundary vertices of an IVW trace from the reference dataset [28], and the connecting grey line shows a typical outline of an IVW bound by these points. Using the length ( $l$ ) and height ( $h$ ) determined from these vertices, the IVW was modelled as a two-dimensional ellipse (solid line and points). Owing to this estimation, the centre of the parcel (COP, centre of the ellipse) was not always located at the intersection of reference  $l$  and  $h$  line segments. Accuracy (AI) was calculated as the ratio of the distance from the centre of the modelled IVW to the prey centre of mass (offset red line,  $d_{\text{prey}}$ ) relative to the distance from the COP to the boundary of the ellipse, through the prey centre of mass (purple line,  $d_{\text{boundary}}$ ), subtracted from one. Predator not drawn to scale. The modelled IVW provides a good approximation of the reference IVW (table 3). (Online version in colour.)

image velocimetry (DPIV) that can be labour intensive, inhibiting large-scale analyses of suction accuracy and understanding its importance for predators.

The IVW contains all particles of water that enter the mouth cavity during a feeding event [30]. The ability to define the IVW is possible because suction forces decay rapidly with distance from the mouth [17,20], limiting the number of particles that are ingested. Ingested particles are tracked back to the frame of mouth opening and encircled, defining the volume within which all particles are ingested [10,28,29]. In this way, the ingested volume represents a summation through time but is visualized spatially in the frame of mouth opening (electronic supplementary material, figure S1). Suction accuracy is then quantified by relating prey position to the centre of the ingested volume (figure 1; [29]). As an effect of particle summation, the length axis represents time, because the first particle ingested is closest to the predator, and the last particle is farthest (relative to the start position). Additionally, the position of maximum height corresponds to the timing of peak gape when suction force is the strongest [17], and 50% of the total volume has been ingested [29]. The greatest suction accuracy should be experienced when prey are located closer to the centre of the IVW, because it maximizes the distance to the edge of the volume, limiting the possibility for prey to escape the volume [30]. By quantifying suction accuracy relative to the centre of the IVW, accuracy reflects both the correct timing and position of the IVW relative to the prey.

This method of quantifying accuracy has helped describe performance differences within and between species [10,28,29]. For example, although *Lepomis macrochirus* (bluegill sunfish) is more accurate, *Micropterus salmoides* (largemouth bass)

generates a larger ingested volume that may be beneficial for capturing evasive prey [29]. Additionally, successful strikes in *Chiloscyllium plagiosum* (white-spotted bamboo sharks) occurred with increased accuracy [10]. However, DPIV limits the variation in both predator accuracy and success, because it requires precisely controlled positions of predator and prey, so that the feeding event is captured within a laser sheet [10,28,29]. This restrictive environment is not representative of natural conditions, and for suction accuracy to be a more applicable performance measure, it is necessary to define a method for estimating shape parameters of the IVW based on non-invasive measurements such as three-dimensional kinematics. Because simple kinematics such as gape, time to peak gape and predator ram speed are indicators of suction performance [19,31], and because the IVW encompasses the particles ingested as a result of suction performance [28,30], these kinematic parameters can also be expected to predict IVW shape parameters such as length and height. We use centrarchid fishes (freshwater sunfishes and basses) to construct a regression-based model of IVW shape to quantify suction accuracy during more natural predator–prey encounters than what can be achieved by using DPIV-based methods.

Centrarchids are a model system for understanding not only the mechanics of suction [17,20,28,31–33], but also the relationships between feeding morphology, performance and ecology [34–40]. This small family contains three primary lineages [41]: *Lepomis* sp. capture small evasive or attached prey with forceful suction [8,38,39], *Micropterus* sp. capture large evasive prey using ram and high-volume suction [8,29,42], and the *Pomoxis* clade, containing the remaining less derived and more generalized genera, capture a range of prey items with relatively unspecialized suction ability

[8,38,39,41]. Suction and ram have traditionally been considered endpoints of a feeding performance continuum [13], and because of their differences in feeding ecology and performance, *L. macrochirus* (bluegill sunfish) and *M. salmoides* (largemouth bass) have been used as model fishes for each behaviour, respectively [8,29,39,43,44]. We will also use these species as representatives of feeding performance extremes, but will include *L. cyanellus* (green sunfish), a species that shares evolutionary history and morphological characteristics with *L. macrochirus*, but is convergent with *M. salmoides* in capturing large evasive prey [38,39,41,42] and represents a potential intermediate level of performance.

Our study has three primary objectives: (i) model the IVW as a spheroid and generate predictive equations of IVW length and height based on data from previously published DPIV studies using *L. macrochirus* and *M. salmoides*. (ii) Apply this model to more natural unrestrained feeding events by quantifying three-dimensional kinematics of *L. macrochirus*, *L. cyanellus* and *M. salmoides* capturing evasive and non-evasive prey. (iii) Determine the relationship between suction accuracy quantified under more natural conditions and capture success. Using this new technique, we show that predators vary in capture success as a result of differences in the size and shape of the suction volume as well as the ability to correctly position and time the suction volume.

## 2. Methods

### 2.1. Modelling the ingested volume

Original data (referred to as reference data) were from previously published DPIV studies that visualized the flow of water into the mouth of feeding *L. macrochirus* (three individuals, 22 trials) and *M. salmoides* (three individuals, 29 trials) [28,29]. Predators were filmed in the lateral perspective capturing tethered prey items. The dimensions of the IVW were determined by manually tracking particles from mouth opening until mouth closing, and a boundary was drawn, in the frame of mouth opening, around particles that crossed the predator's jaws and were ingested (figure 1 grey boundary and the electronic supplementary material, figure S1). Further details on these methods are published elsewhere [17,28,29].

From these trials, the digitized positions of the top, bottom, left and right vertices of the boundary in the midsagittal plane of the predator (figure 1, grey open circles) were used to calculate maximum IVW height ( $h$ , cm) and length ( $l$ , cm) and the ratio of height : length ( $H : L$ ). The centre of mass of the parcel (COP) was used to calculate the distance to the prey ( $d_{\text{prey}}$ , cm) and distance to the boundary through the prey centre of mass ( $d_{\text{boundary}}$ , cm). Accuracy index (AI; table 1) was calculated using the following equation (figure 1):

$$\text{AI} = 1 - \left( \frac{d_{\text{prey}}}{d_{\text{boundary}}} \right), \quad (2.1)$$

where  $\text{AI} = 1$  indicated prey were located at the centre of the IVW and  $\text{AI} < 0$  indicated prey were located outside of the boundary. Kinematics, including ram speed (predator velocity taken at the time of peak gape,  $\text{cm s}^{-1}$ ), peak gape height (greatest distance between upper and lower jaws, cm) and time to peak gape height (TTPG; time from mouth opening to peak gape height, ms), were calculated for each trial. All of these data were quantified in previously published work, but are available in supplemental material uploaded to Dryad (doi:10.5061/dryad.hf591).

To model the IVW, we simplified the shape and then predicted the dimensions using kinematics. An ellipse was used to approximate the rounded shape of the IVW in the midsagittal

**Table 1.** List of symbols and abbreviations<sup>a</sup>.

symbol	definition
AI	accuracy index
$\text{AI}_x$	accuracy index in the $x$ -dimension
$\text{AI}_y$	accuracy index in the $y$ -dimension
$\text{AI}_z$	accuracy index in the $z$ -dimension
COP	centre of the parcel of water
$d_{\text{boundary}}$	distance from the COP to the intersection with the IVW boundary, through the prey centre of mass (cm)
$d_{\text{prey}}$	distance from the COP to the prey centre of mass (cm)
$h$	maximum IVW height, reference dataset (cm)
$h_p$	predicted IVW height, from multiple regression (cm)
$H : L$	height : length ratio
IVW	ingested volume of water
$l$	maximum IVW length, reference dataset (cm)
$l_p$	predicted IVW length, from multiple regression (cm)
$P$	estimated probability of capture success
TTPG	time to peak gape height, from mouth opening to peak gape (ms)
$w_p$	predicted three-dimensional IVW width, equal to $h_p$ (cm)

<sup>a</sup>Table does not include symbols used in the electronic supplementary material.

plane of the predator [17,18,28,29]. Each IVW variable was then calculated using  $l$  and  $h$  as the major and minor axes of an ellipse, respectively (for details, see electronic supplementary material, Methods), and variables were compared with the reference data using Student's  $t$ -test to validate that the elliptical IVW was similar to that of the reference IVW for each species. Following validation of the IVW shape, multiple linear regressions were used to predict IVW height ( $h_p$ ) and length ( $l_p$ , dependent variables) from ram speed, peak gape height and TTPG (independent variables), so that ellipse dimensions could be obtained without the use of DPIV. Because species were chosen to bracket the range of functional performance and prediction equations that are applicable for any species within the observed kinematic range are more useful, multiple linear regressions were carried out at the sample unit of trials ( $n = 52$  trials). All possible combinations of kinematic variables were included as independent variables, and statistical models were compared using corrected Akaike information criteria (AICc) values [45,46]. Because the difference between models can be small, Akaike weights ( $w_i$ ) were calculated to assess the probability that the best model was the best given the other models, and evidence ratios (ERs) were calculated to determine how many times greater the best model was compared with other models [45,46]. Models with  $\text{ER} > 3$  had little support. All calculations were performed in Matlab (R2010a, The MathWorks, Inc., Natick, MA), and code for performing these analyses can be found on the primary author's personal website. All statistics were performed in JMP (ver. 10.0, SAS Institute, Inc., Cary, NC).

### 2.2. Quantifying accuracy under unrestrained conditions

#### 2.2.1. Three-dimensional kinematics

To expand the accuracy metric to more natural behaviours, where predator and prey could respond in any direction,

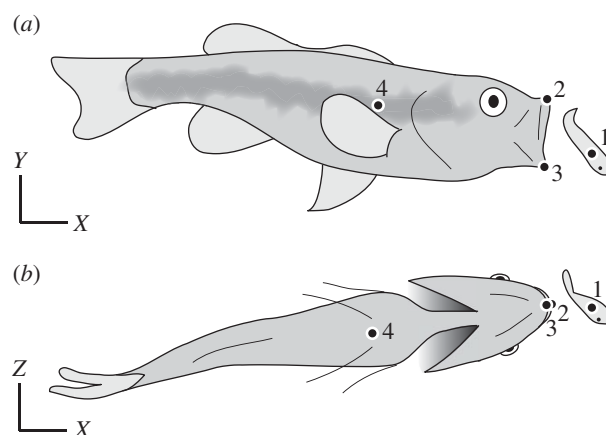
**Table 2.** Species, sample sizes and capture success rates for three-dimensional kinematic dataset. SL, standard length;  $n$ , sample size for statistical analyses on three-dimensional kinematic data. Values are mean  $\pm$  s.d.

	<i>Lepomis macrochirus</i>	<i>Lepomis cyanellus</i>	<i>Micropterus salmoides</i>
mean SL (cm)	8.88 $\pm$ 0.91	6.57 $\pm$ 0.74	7.72 $\pm$ 2.79
mean body mass (g)	21.11 $\pm$ 5.67	9.90 $\pm$ 4.32	10.46 $\pm$ 12.42
capture success (%)	93.8 (non-evasive) 68.6 (evasive)	96.4 (non-evasive) 63.6 (evasive)	96.5 (non-evasive) 95.8 (evasive)
no. trials performed	134	119	105
no. individuals analysed	5	3	5
no. trials analysed (by individual), non-evasive	5, 5, 5, 5, 5 ( $n = 25$ trials)	5, 5, 5 ( $n = 15$ trials)	5, 5, 5, 5, 4 ( $n = 24$ trials)
no. trials analysed (by individual), evasive	5, 5, 6, 5, 5 ( $n = 26$ trials)	4, 6, 4 ( $n = 14$ trials)	5, 5, 6, 5, 5 ( $n = 26$ trials)
no. evasive trials analysed that were missed capture attempts (by individual)	2, 2, 2, 0, 2	1, 3, 1	0, 0, 1, 0, 0

three-dimensional analyses were necessary and comprise original data used to assess differences in accuracy and success among predators. Individuals were collected from Issaqueena Lake, Clemson University Experimental Forest, Clemson, SC (table 2). Specimens were housed individually in 38 l aquaria maintained at 24°C, and were fed daily with commercially available frozen invertebrates (bloodworms, mosquito larvae, pieces of frozen shrimp) or live fish (wild-type sailfin mollies, *Poecilia latipinna*). Fish were transferred to a 75 l filming tank and allowed to acclimate for 1–2 days, during which time food was withheld. The Institutional Animal Care and Use Committees at Clemson University and the University of California, Riverside approved all experimental procedures.

Individuals were recorded at 500 fps (1080  $\times$  1080 pixels, Photron APX-RS, Photron USA Inc., San Diego, CA) using two cameras to record lateral and ventral views (figure 2) while capturing non-evasive free-floating cut pieces of shrimp or evasive live untethered mollies (filming volume 53  $\times$  32  $\times$  29 cm). These prey items were chosen to elicit a range of prey capture behaviours that encompassed previously collected DPIV behaviours [28,29] as well as maximum performance behaviours, and both prey items were scaled to predator mouth size. Capture success was determined by scoring all trials as either a capture or miss, where misses were classified as trials in which the prey centre of mass did not cross the boundary of the predator's jaws, and was determined visually after each trial. Trials in which the predator missed and then captured the prey in a subsequent attempt were scored as a miss. For each species capturing evasive prey, a combination of successful and unsuccessful trials were chosen for analysis to represent the overall capture success observed in each species (table 2).

Trials were digitized (figure 2) using DLTdv3 [47] in Matlab, and all points were smoothed using a lowpass butterworth filter with a 60 Hz cut-off frequency (as in reference [48]). This value was chosen by evaluating smoothing results across a range of values for several representative videos. Smoothing was verified visually for each trial to ensure the precision of smoothed values. The midpoint of the mouth aperture was the average three-dimensional position of both the upper and lower jaws, and was used to position the IVW relative to the predator and prey (electronic supplementary material, Methods). The following kinematics were analysed using the smoothed digitized points: prey velocity (mean velocity of estimated prey centre of mass prior to

**Figure 2.** Digitized three-dimensional anatomical landmarks shown on a trace of a representative *M. salmoides* trial for the (a) lateral and (b) ventral views. 1, approximate prey centre of mass; 2, tip of predator upper jaw; 3, tip of predator lower jaw and 4, approximate predator centre of mass.

movement induced by suction,  $\text{cm s}^{-1}$ ), peak gape height (maximum distance between the upper and lower jaws, cm), TTPG (elapsed time between mouth opening and peak gape, ms) and ram speed (change in predator centre of mass position divided by the change in time between frames, taken at the time of peak gape,  $\text{cm s}^{-1}$ ). Studies on centrarchids typically define mouth opening as 20–95% of peak gape owing to variable mouth opening and asymptotic gape height [17,28,29], but here neither of these conditions was apparent.

## 2.2.2. Applying the ingested volume of water model to three-dimensional dynamic capture events

AI was calculated by determining the three-dimensional distance between the COP and the prey, and relating this to the three-dimensional distance between the COP and the IVW boundary (through the prey centre of mass) as in equation (2.1). For details regarding modifications of the model for three dimensions and calculation of the boundary intersection point, see the electronic supplementary material, Methods. As in previous work [29], AI was also calculated in each dimension. Ingested volume ( $\text{cm}^3$ )

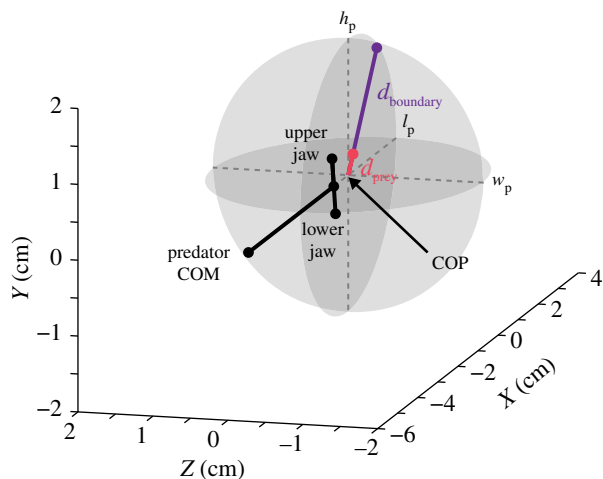


**Figure 3.** Three-dimensional reconstruction of a representative *L. macrochirus* trial showing the positions of predator (large black dots) and prey (red dot) landmarks at 4 ms prior to prey capture. The estimated ingested volume of water (IVW) is overlain using grey shaded ellipses representing  $X$ ,  $Y$  and  $Z$  dimensions. Predicted height ( $h_p$ ), length ( $l_p$ ) and width ( $w_p$ ) of the volume are shown with dashed grey lines. Accuracy is calculated following figure 1, where  $d_p$  (red line) is the three-dimensional distance to the prey and  $d_b$  (purple line) is the three-dimensional distance to the spheroid boundary through the prey centre of mass. This figure was generated from trial for which sample data are available in the electronic supplementary material. Parameters for this trial are as follows: ram  $86.5 \text{ cm s}^{-1}$ , gape  $1.06 \text{ cm}$ , time to peak gape  $32 \text{ ms}$ , mean prey velocity  $13.5 \text{ cm s}^{-1}$ ,  $l_p$   $4.78 \text{ cm}$ ,  $h_p$ ,  $w_p$   $3.62 \text{ cm}$ , H:L  $0.76$ ,  $d_p$   $0.30 \text{ cm}$ ,  $d_b$   $1.81 \text{ cm}$ , AI  $0.83$ , ingested volume  $32.68 \text{ cm}^3$ . (Online version in colour.)

was quantified using the ellipsoid volume equation

$$\text{Ingested volume} = \left(\frac{4\pi}{3}\right) * (l_p * w_p * h_p). \quad (2.2)$$

All kinematic analyses and calculations were performed in Matlab. Supplemental material uploaded to Dryad (doi:10.5061/dryad.hf591) includes a sample video for the trial used to generate figure 3 and smoothed digitized points for this video. Matlab code for analysing this trial can be found in a .zip file on the primary author's personal website, which also includes the smoothed digitized points data.

The combinations of species and prey type were chosen to represent the range of functional variation across centrarchids (suction, ram and intermediate feeding specialization; high and low performance), and statistical analysis used these functional groups (e.g. combinations of species and prey type such as *L. macrochirus* with evasive prey) rather than nesting prey type within species. Individual variation was significant only for H:L in *M. salmoides* (Kruskal–Wallis, individuals within species as independent variable,  $\chi_1^2 = 18.39$ ,  $p = 0.0010$ ) and was not significant for any other three-dimensional IVW parameter ( $p > 0.21$ ). Therefore, the effect of individual was considered insignificant, and trials within each functional group were used as the sampling units (table 2;  $n = 14$ – $26$  trials for each (species  $\times$  prey type) functional group).

Means were calculated for H:L, ingested volume, AI and AI in each dimension, inclusive of misses, for each functional group. Assumptions of normality and equal variance within each functional group were tested with Shapiro–Wilk's and Levene's tests, respectively. Neither of these assumptions was met by all functional groups, and non-parametric Kruskal–Wallis tests were performed with H:L, ingested volume, AI or AI in each dimension

as dependent variables and functional groups as independent variables. These were followed with post hoc Dunn's multiple comparison tests to determine which groups were significantly different. Means are given with standard error except when indicated. All statistics were performed in JMP.

### 2.3. The relationship to capture success

To determine the relevance of predator accuracy to prey capture behaviours, a logistic regression was performed between capture success (binary dependent variable) and AI (continuous independent variable). As with the equations for predicting IVW height and length, the interest was in predictive capability across the range of prey capture behaviours among species, and logistic regression analyses were performed on evasive prey trials without accounting for species or individual ( $n = 66$  trials). Logistic regression was performed using Matlab.

## 3. Results

### 3.1. A regression-based ingested volume of water model

No significant differences in the parameters of H:L and AI were found between reference and modelled volumes, and an ellipse captured the geometry of the IVW in the midsagittal plane of the predator (table 3). In the absence of known IVW vertices, height of the IVW was predicted using predator ram speed and peak gape height (table 4) with the equation

$$h_p = 0.670 + (0.018 * \text{ram}) + (1.311 * \text{gape}). \quad (3.1)$$

The best regression model for predicting IVW length only included ram speed. However, if ram speed is  $0 \text{ cm s}^{-1}$  (it is possible for predators to use suction with no forward movement), then this would result in predicting a constant IVW length across a range of species and behaviours. Therefore, we chose to use the second best model for further analyses, which included both ram and gape (table 4) with the equation

$$l_p = 0.927 + (0.037 * \text{ram}) + (0.611 * \text{gape}). \quad (3.2)$$

This model explained a similar amount of variation as the best model without gape (table 4), and although it did result in  $l_p$  values that significantly decreased by  $0.34$ – $0.45 \text{ cm}$  and significantly more circular ingested volumes, it did not result in differences in AI across species (electronic supplementary material, table S1). Because predators must open their mouths to generate suction, and because mouth size reflects the capacity to generate suction [43], including gape in the regression equations essentially scaled the IVW to the predator's mouth size. Time to peak gape was not included in the best fitting model for either  $h_p$  or  $l_p$  (table 4). Both regression models (for  $h_p$  and  $l_p$ ) explained a significant portion of the variation in the reference values of each parameter ( $h_p$ : ANOVA,  $F_{2,48} = 64.04$ ,  $p < 0.0001$ ;  $l_p$ : ANOVA,  $F_{2,48} = 123.31$ ,  $p < 0.0001$ ), and the predicted values were similar to the actual values calculated using the reference dataset (figure 4).

### 3.2. Applying suction accuracy to more natural three-dimensional trials

Success was high for all species when capturing non-evasive prey, but varied when capturing evasive prey (table 2).

**Table 3.** Student's *t*-test for reference and modelled IVW parameters. H:L, height: length;  $d_{\text{prey}}$ , distance to the prey;  $d_{\text{boundary}}$ , distance to the boundary; AI, accuracy index. Values for reference and modelled IVW are mean  $\pm$  s.e. No variables are significantly different ( $\alpha = 0.05$ ).

variable	species	reference	modelled	<i>t</i>	<i>p</i>
H:L	<i>L. macrochirus</i>	1.15 $\pm$ 0.03	1.16 $\pm$ 0.03	-0.17	0.87
	<i>M. salmoides</i>	1.02 $\pm$ 0.03	1.00 $\pm$ 0.03	0.28	0.78
$d_{\text{prey}}$	<i>L. macrochirus</i>	0.21 $\pm$ 0.03	0.26 $\pm$ 0.03	-1.25	0.22
	<i>M. salmoides</i>	1.01 $\pm$ 0.06	0.88 $\pm$ 0.06	1.49	0.14
$d_{\text{boundary}}$	<i>L. macrochirus</i>	1.03 $\pm$ 0.04	1.00 $\pm$ 0.04	0.62	0.54
	<i>M. salmoides</i>	1.89 $\pm$ 0.07	1.93 $\pm$ 0.06	-0.44	0.66
AI	<i>L. macrochirus</i>	0.80 $\pm$ 0.02	0.74 $\pm$ 0.03	1.82	0.08
	<i>M. salmoides</i>	0.46 $\pm$ 0.03	0.54 $\pm$ 0.03	-1.84	0.07

**Table 4.** Multiple linear regression model selection statistics for predicting IVW height and length using the reference dataset. Predictors are ordered by AIC<sub>c</sub> value. TTPG, time to peak gape height; DF, degrees of freedom; SSE, error sum of squares; RMSE, root mean squared error; AIC<sub>c</sub>, corrected Akaike information criterion;  $w_i$ , Akaike weight; ER, evidence ratio.

	parameters estimated	d.f.	SSE	RMSE	adjusted $R^2$	AIC <sub>c</sub>	$w_i$	ER
<i>predictors of IVW height</i>								
ram + gape	3	48	11.97	0.50	0.72	79.67 <sup>a,b</sup>	0.70	1.00
ram + gape + TTPG	4	47	11.95	0.50	0.71	82.08	0.10	6.93
ram	2	49	13.68	0.53	0.68	84.14	0.17	4.25
ram + TTPG	3	48	13.57	0.53	0.68	86.08	0.03	24.61
gape	2	49	16.30	0.58	0.62	93.07	0.00	370.34
gape + TTPG	3	48	16.14	0.58	0.62	94.91	0.00	2036.50
TTPG	2	49	41.01	0.91	0.05	140.12	0.00	6.10 $\times 10^{12}$
<i>predictors of IVW length</i>								
ram	2	49	14.47	0.54	0.83	87.00 <sup>a</sup>	0.66	1.00
ram + gape	3	48	14.10	0.54	0.83	88.03 <sup>b</sup>	0.18	3.67
ram + TTPG	3	48	14.34	0.55	0.83	88.88	0.12	5.62
ram + gape + TTPG	4	47	13.72	0.54	0.83	89.12	0.05	13.17
gape	2	49	33.21	0.82	0.61	129.36	0.00	1.58 $\times 10^9$
gape + TTPG	3	48	31.73	0.81	0.62	129.40	0.00	3.54 $\times 10^9$
TTPG	2	49	83.41	1.30	0.02	176.33	0.00	2.50 $\times 10^{19}$

<sup>a</sup>Best choice model (smallest AIC<sub>c</sub>).<sup>b</sup>Model used in further analyses (see Results section 3.1).

Although *M. salmoides* had similarly high success rates with both prey types, both *L. macrochirus* and *L. cyanellus* decreased success rates by 25.2% and 32.8%, respectively, when capturing evasive prey. Differences across prey types were also apparent with kinematics (table 5). Ram speeds ranged from 22.1  $\pm$  2.4 cm s<sup>-1</sup> in *L. macrochirus* capturing non-evasive prey to 114.3  $\pm$  4.9 cm s<sup>-1</sup> in *M. salmoides* capturing evasive prey and peak gape height ranged from 0.83  $\pm$  0.05 cm to 1.21  $\pm$  0.07 cm in the same species and prey types. Therefore, these functional groups represent observed extremes in kinematic performance in this study. Ram speed and peak gape height in *L. cyanellus* were intermediate to the other species when capturing evasive prey, but were both greater than the other species for non-evasive prey, indicating that performance differences between prey types was not as dramatic in *L. cyanellus*.

Kinematic differences led to significant differences in the shape (H:L; Kruskal-Wallis,  $\chi^2_5 = 63.34$ ,  $p < 0.0001$ ) and size (ingested volume; Kruskal-Wallis,  $\chi^2_5 = 76.90$ ,  $p < 0.0001$ ) of the IVW (table 5). The ratio of H:L ranged from 0.74  $\pm$  0.015 (elongate) for *M. salmoides* capturing evasive prey to 0.96  $\pm$  0.015 (nearly circular) for *L. macrochirus* capturing non-evasive prey, supporting the idea that these two functional groups represent extremes in performance. Additionally, the H:L of *L. macrochirus* capturing non-evasive prey was significantly greater than any species capturing evasive prey, and *L. cyanellus* was the only species where H:L was not different across prey types (figure 5). Differences in size of the ingested volume mirrored those observed for H:L. The greatest ingested volume was observed for *M. salmoides* capturing evasive prey and was greater than all other functional groups with the exception of

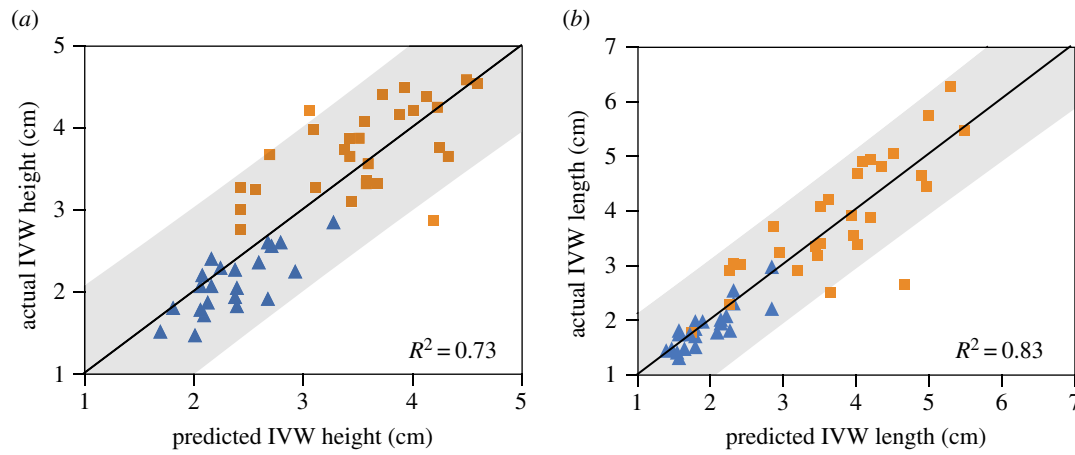


**Figure 4.** The relationship between predicted and actual values (from the reference dataset) of IVW (a) height and (b) length. Height and length were predicted using multiple linear regressions with ram speed and gape height as predictors (table 4). *L. macrochirus* trials are shown with blue triangles and *M. salmoides* trials are shown with orange squares. The regression line and 95% prediction intervals are also shown with a black line and grey shading, respectively. These intervals indicate the ability to obtain each actual value at a given predicted value. (Online version in colour.)

**Table 5.** Mean three-dimensional kinematics and modelled IVW parameters for each species and prey type. NE, non-evasive prey; E, evasive prey; TTPG, time to peak gape height,  $h_p$ , predicted height;  $l_p$ , predicted length; H:L, height: length ratio; AI, accuracy index;  $AI_x$ , accuracy along the x-axis;  $AI_y$ , accuracy along the y-axis;  $AI_z$ , accuracy along the z-axis. Values are mean  $\pm$  s.e. Significant differences among means are discussed in the text and figure 5.

variable	<i>L. macrochirus</i>		<i>L. cyanellus</i>		<i>M. Salmoides</i>	
	NE	E	NE	E	NE	E
ram ( $\text{cm s}^{-1}$ )	22.08 $\pm$ 2.4	68.00 $\pm$ 5.3	65.13 $\pm$ 9.2	89.61 $\pm$ 6.6	47.81 $\pm$ 7.4	114.29 $\pm$ 4.9
gape (cm)	0.83 $\pm$ 0.05	1.05 $\pm$ 0.03	1.00 $\pm$ 0.04	1.08 $\pm$ 0.05	0.90 $\pm$ 0.07	1.21 $\pm$ 0.07
TTPG (ms)	53.8 $\pm$ 3.6	28.3 $\pm$ 1.2	31.9 $\pm$ 2.8	28.9 $\pm$ 2.5	30.5 $\pm$ 2.5	25.1 $\pm$ 2.1
$h_p$ (cm)	2.15 $\pm$ 0.09	3.28 $\pm$ 0.11	3.16 $\pm$ 0.20	3.69 $\pm$ 0.17	2.71 $\pm$ 0.19	4.31 $\pm$ 0.11
$l_p$ (cm)	2.25 $\pm$ 0.11	4.09 $\pm$ 0.20	3.95 $\pm$ 0.35	4.90 $\pm$ 0.27	3.25 $\pm$ 0.30	5.89 $\pm$ 0.17
H:L	0.96 $\pm$ 0.015	0.82 $\pm$ 0.014	0.83 $\pm$ 0.025	0.76 $\pm$ 0.009	0.86 $\pm$ 0.020	0.74 $\pm$ 0.015
$d_{\text{prey}}$ (cm)	0.23 $\pm$ 0.023	0.90 $\pm$ 0.125	0.48 $\pm$ 0.077	0.90 $\pm$ 0.202	0.43 $\pm$ 0.061	0.62 $\pm$ 0.061
$d_{\text{boundary}}$ (cm)	1.10 $\pm$ 0.05	1.85 $\pm$ 0.10	1.83 $\pm$ 0.15	2.15 $\pm$ 0.14	1.55 $\pm$ 0.15	2.62 $\pm$ 0.08
AI	0.79 $\pm$ 0.02	0.51 $\pm$ 0.07	0.74 $\pm$ 0.03	0.59 $\pm$ 0.10	0.73 $\pm$ 0.02	0.77 $\pm$ 0.02
$AI_x$	0.88 $\pm$ 0.02	0.69 $\pm$ 0.05	0.81 $\pm$ 0.04	0.72 $\pm$ 0.09	0.80 $\pm$ 0.02	0.83 $\pm$ 0.03
$AI_y$	0.90 $\pm$ 0.02	0.76 $\pm$ 0.05	0.91 $\pm$ 0.02	0.86 $\pm$ 0.03	0.90 $\pm$ 0.01	0.91 $\pm$ 0.01
$AI_z$	0.91 $\pm$ 0.02	0.80 $\pm$ 0.05	0.94 $\pm$ 0.02	0.79 $\pm$ 0.06	0.91 $\pm$ 0.02	0.95 $\pm$ 0.01
ingested volume ( $\text{cm}^3$ )	6.3 $\pm$ 0.9	25.6 $\pm$ 3.2	25.2 $\pm$ 5.5	38.5 $\pm$ 6.1	18.2 $\pm$ 4.8	59.9 $\pm$ 4.4

*L. cyanellus* capturing evasive prey. The smallest volume predicted, that of *L. macrochirus* capturing non-evasive prey, was only 21.1% of the size of the largest volume. Again, *L. cyanellus* was the only species for which there were no significant differences in ingested volume across prey types. These differences in IVW shape and size are apparent when the mean IVW is visualized (figure 6 and electronic supplementary material, figure S2).

AI was generally high across functional groups with a maximum of  $0.79 \pm 0.02$  in *L. macrochirus* capturing non-evasive prey. However, although there were significant differences (Kruskal–Wallis,  $\chi^2_5 = 19.83$ ,  $p = 0.0013$ ), these were few (figure 5). Specifically, *L. macrochirus* capturing evasive prey had the poorest accuracy, and this was significantly lower than both *L. macrochirus* capturing non-evasive prey and *M. salmoides* capturing evasive prey (Dunn's multiple

comparison tests,  $z > 3.07$ ,  $p < 0.03$ ). For both piscivores, although AI was reduced with evasive prey, this difference was not significant (Dunn's multiple comparison tests, *L. cyanellus*,  $z = 1.362$ ,  $p = 1.00$ , *M. salmoides*,  $z = -0.896$ ,  $p = 1.00$ ). In examining AI in each dimension, significant differences were observed only in the X- (Kruskal–Wallis,  $\chi^2_5 = 12.45$ ,  $p = 0.0291$ ) and Z-dimensions (Kruskal–Wallis,  $\chi^2_5 = 20.72$ ,  $p = 0.0009$ ). Specifically,  $AI_x$  was greater for *L. macrochirus* capturing non-evasive prey than for the same species capturing evasive prey (Dunn's multiple comparison tests,  $z = 3.30$ ,  $p = 0.0146$ ). Additionally,  $AI_z$  was greater for *M. salmoides* capturing evasive prey than either other species with the same prey (Dunn's multiple comparison tests, *L. macrochirus*,  $z = 3.33$ ,  $p = 0.013$ , *L. cyanellus*,  $z = 3.70$ ,  $p = 0.0032$ ). For all functional groups, accuracy was poorest in the X-dimension, along the path of forward trajectory

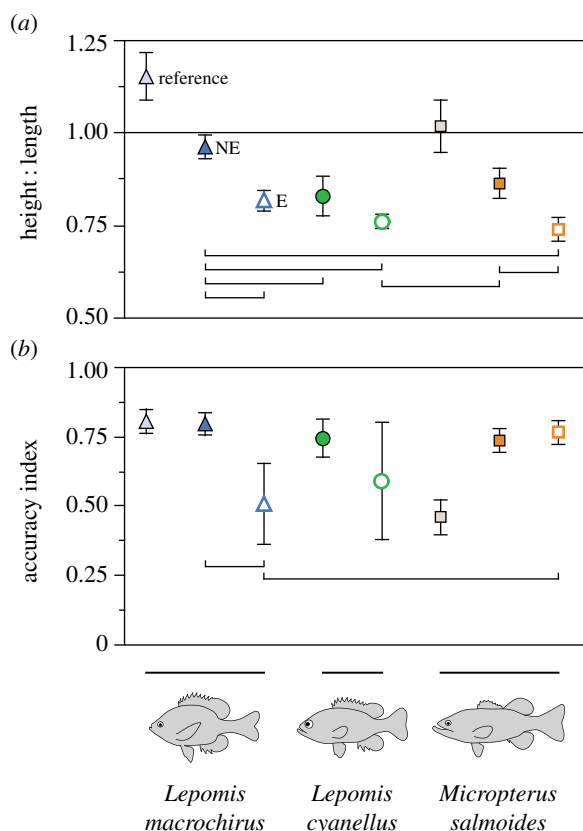


**Figure 5.** Species means and 95% CIs for (a) H:L ratio and (b) accuracy index. Comparisons are shown for two-dimensional reference data obtained with particle image velocimetry techniques [28,29] for *Lepomis macrochirus* and *M. salmoides* (shown for comparison, light filled shapes), as well as for three-dimensional modelled estimates for all three species capturing non-evasive (NE; unfilled shapes) and evasive (E; dark filled shapes) prey types. A line is drawn at H:L = 1 to indicate the value at which the ingested volume of water is circular. General body shape is also shown for each species. Significant differences are indicated by brackets, where functional groups that are linked are significantly different (Dunn's multiple comparison tests,  $p < 0.02$ ). (Online version in colour.)

(table 5), non-evasive prey were located closer to the COP than evasive prey, and prey that were missed were positioned farther from the COP than successful captures (figure 5).

### 3.3. Accuracy and capture success

AI explained 52.7% of capture success. The estimated probability of success ( $P$ ) can be predicted using the equation

$$\ln\left(\frac{P}{1-P}\right) = -5.059 + (11.038 * AI). \quad (3.3)$$

The odds ratio was calculated by scaling the regression coefficient for AI by the standard deviation (s.d.) for AI (s.d. = 0.30). Predators were 30 times more likely to successfully capture prey with a standard deviation increase in AI. Strikes where AI was less than 0 (indicating prey were located outside the modelled IVW boundary) always resulted in missed capture attempts (figure 7).

## 4. Discussion

We present a novel method to determine predator accuracy in suction-feeding fishes by predicting the shape of the IVW and relating prey position to the centre of this volume in three

dimensions. Unlike prior methods [10,29], our model can be used when predator and prey are unconstrained, which more closely matches natural predator-prey interactions. Additionally, this model only requires kinematics, and is therefore more efficient for analysing a large number of individuals and/or species. We applied this model to more natural prey capture events for three species of closely related predators capturing evasive and non-evasive prey and show that accuracy predicts success. Our model makes IVW parameters and suction accuracy more accessible measures of prey capture performance that can be used to understand predator strategies and generate large-scale hypotheses of prey capture performance evolution.

### 4.1. Model performance and limitations

Our model of the IVW was used to quantify suction accuracy under more natural conditions, and significantly explained more than 50% of the variation in capture success. Therefore, our model is a reasonable estimate of the ability for predators to correctly position and time their strike relative to the prey [6]. However, in comparison with previously published work using DPIV analyses, differences in accuracy between species were not replicated. Although *L. macrochirus* (AI = 0.80) was 74% more accurate than *M. salmoides* (AI = 0.46) [29], in this study, the trend was reversed, particularly with evasive prey: *M. salmoides* (AI = 0.77) was 51% more accurate than *L. macrochirus* (AI = 0.51). This indicates that the experimental techniques used in each study may present bias towards the feeding behaviours of each species. Because *L. macrochirus* is specialized for capturing attached prey with forceful suction [8,38,39], presenting predators with tethered prey could artificially inflate the performance of *L. macrochirus* relative to *M. salmoides*. Alternatively, presenting predators with free-swimming evasive fishes, as in this study, could favour the strategy of *M. salmoides*. Therefore, future studies should include multiple prey types to accurately account for specialization among species. Specifically, we suggest the three prey types defined in Holzman [8]: large evasive, small evasive and attached prey. Each of these prey types requires divergent functional demands, and these demands have been demonstrated as axes of diversification among centrarchids [8,39,42].

Our model of the IVW and estimates of accuracy predict capture success and support the use of accuracy as a performance measure [7], and it is a necessary link for understanding suction performance. Some of the earliest models of suction behaviours were useful for describing the detailed hydrodynamics of suction feeding [15,16,49,50], but none of these models addresses whether the event results in successful capture. Two approaches have recently been developed to understand differences in capture success across suction-feeding predators: the suction-induced flow field (SIFF) model [8], and accuracy relative to the IVW [10,29]. The SIFF model uses kinematics, fluid flow and prey characteristics to predict hydrodynamic forces experienced by prey as a measure of a predator's ability to entrain a prey item [8]. Although SIFF simplifies predator-prey interactions and predicts what species should be capable of, the IVW model relies on trial-level kinematics to understand what actually happens during a feeding event. Therefore, these two models are complimentary—SIFF predicts capture success and the IVW model explains capture success with

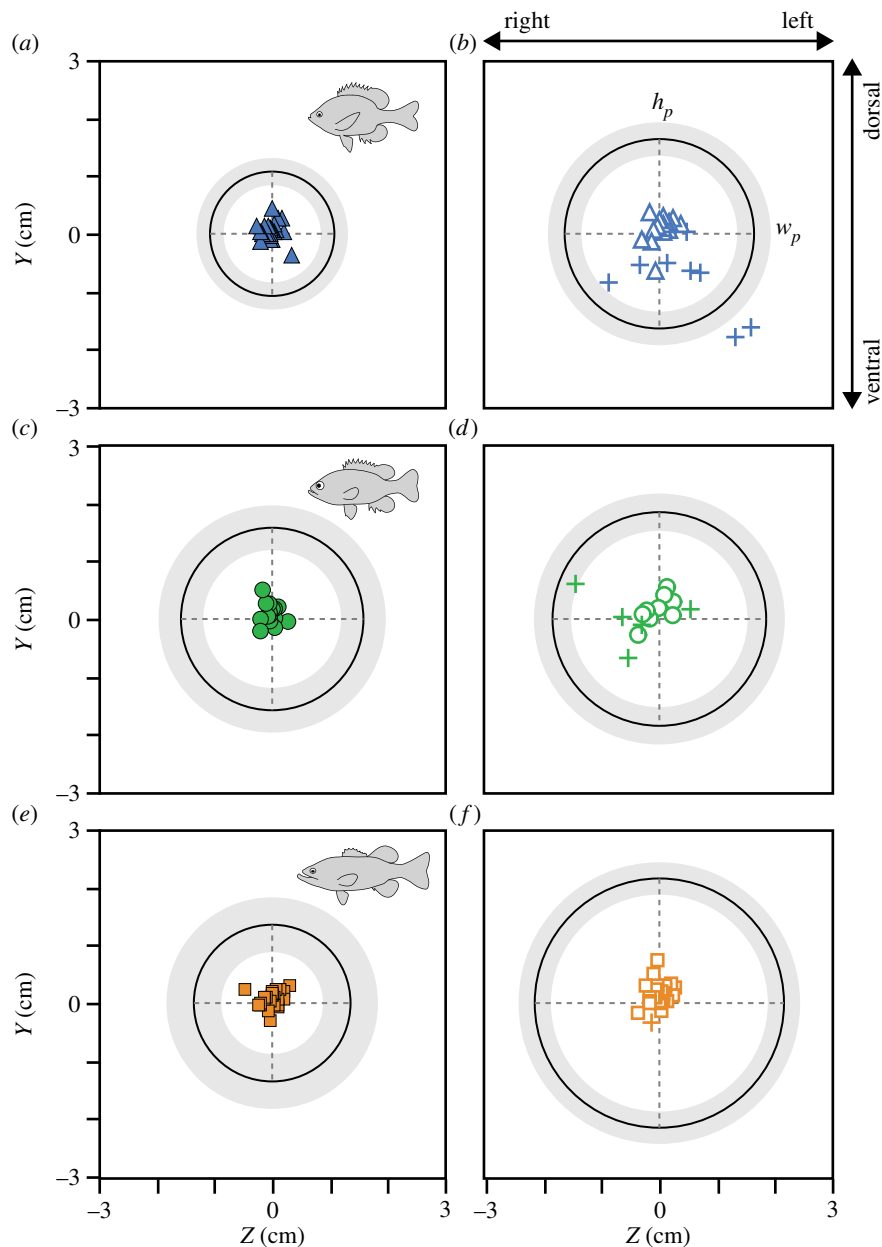


**Figure 6.** Position of prey relative to the modelled IVW in the frontal view of the predator, shown for (a,b) *L. macrochirus*, (c,d) *L. cyanellus* and (e,f) *M. salmoides* capturing non-evasive (a,c,e) and evasive (b,d,f) prey types. Markers follow figure 5 with the addition of missed prey capture attempts shown as plus symbols. Prey positions are plotted for each trial, with an ellipse that represents the mean  $\pm$  s.d. (black line and grey shading, respectively) IVW shape for each functional group. This visualization represents the predator approaching toward the viewer. Predicted height ( $h_p$ ) and width ( $w_p$ ) axes are also shown. (Online version in colour.)

accuracy. By expanding on the DPIV technique to capture a wider range of predatory behaviours, our IVW-based model of suction performance represents a significant step towards linking feeding performance with feeding success, and can be used to better understand why suction-feeding predators are more or less successful on divergent prey types.

All models are simplifications of natural phenomena, and as such, impose limitations on their interpretations and applicability. Our IVW model has three primary assumptions: (i) that modifications of the IVW are the primary means of modulating accuracy, (ii) that an ellipsoid (or more technically, a spheroid) approximates the ingested volume and (iii) that prey positioned closer to the COP represents greater accuracy. Predators can control the position of the IVW relative to the prey by protruding their jaws at an angle, thereby deflecting the IVW in the respective direction (as in sharks [10]), by altering their orientation during the approach to the prey (personal observation 2013), or by modifying the

hydrodynamics to affect the reach and volume of suction [29]. Because the species we used have terminal mouths, we assume deflection was negligible. We also assume that by the time of the strike the predator has completed its orientation behaviours to facilitate the use of lateral musculature for powering mouth expansion [43,51]. Our work supports the second assumption that an ellipse approximates the shape of the ingested volume in the midsagittal plane of the predator based on two-dimensional, constrained prey capture events, but this may not be the case if mouth shape is not circular at all points of mouth opening (as indicated in [30]) or if predator direction varies during the strike (e.g. pitch during braking). However, it is difficult to visualize three-dimensional hydrodynamics of suction in moving predators at this time, and this simplified model provides reasonable estimates that can be fine-tuned given further developments. The final assumption regarding the position within the volume representing the greatest accuracy has

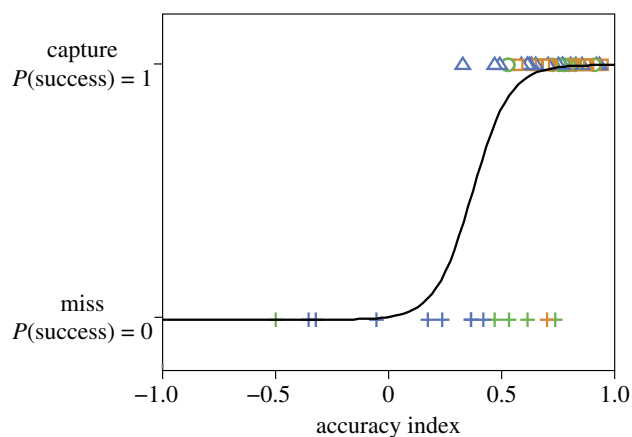


**Figure 7.** Logistic regression of the probability of capture success against accuracy index for three-dimensional modelled trials. Accuracy explains 52.7% of capture success. Marker style follows figure 6. (Online version in colour.)

never been addressed, but we provide data indicating that it may not be entirely correct.

Studies that have quantified suction accuracy using the IVW have assumed that the greatest accuracy occurs when prey are located at the COP [10,29]. However, this has never been verified by statistically testing whether position along any axis affects success. It can be argued that for prey items that are located at 25% and 75% of the length of the  $x$ -axis, projected forward of the predator along the centreline (figure 3), AI would be 0.5 in both cases, but the prey at 25% would be encountered prior to peak gape, whereas the prey at 75% would be encountered after. This gives the predator a greater chance of capturing the prey at 25% compared with the one at 75%. Using our data on capture success, we calculated the position of the prey as a percentage along the  $x$ ,  $y$ , and  $z$  axes and performed logistic regressions to determine whether success was biased by prey position along any axis. We found that predators have an increased chance of success when prey are located closer to the predator on the  $x$ -axis and higher in the volume on the  $y$ -axis. There was no effect of position along the  $z$ -axis (predator's left versus right) on predator success (electronic supplementary material, figure S3). Therefore, had our measure of accuracy accounted for these biases towards success, we may have found a stronger relationship between accuracy and success. However, because we were able to establish a relationship between accuracy and success, the effect of this bias may only be slight. This represents a significant caveat to our model, and future work should address a method for accounting for positional biases when quantifying accuracy.

This study was performed on adult fishes where viscous forces are negligible during prey capture and suction flow is unidirectional, and therefore our model has limited applications for small or larval fishes where viscous forces could have a significant effect on suction performance (Reynold's number  $< 200$ ) [52,53] or secondarily aquatic vertebrates where suction flow is bidirectional [54,55]. Note also that as predator size reaches its lower extreme in larval fishes, mouth size and ram speed may approach 0 and the predicted length and height of the IVW might converge towards 0.967 and 0.670, but this relationship between IVW length and height at small predator sizes has not been verified. However, our model can be applied to the majority of cases and is therefore appropriate as a starting point. Centrarchids were chosen in this study owing to the extensive body of research supporting hydrodynamic and kinematic relationships, but

additional taxa should also be assessed and tested against DPIV analyses to verify the applicability of our model to other species. The utility of the IVW model comes from the ability to assess performance across a range of suction-feeding predators and to generate macroevolutionary hypotheses of prey capture evolution.

## 4.2. Factors that affect suction accuracy

Holzman *et al.* [8, p. 8] outline three primary factors determining the outcome of a suction-feeding predation attempt: the predator's strategy for approaching prey, the predator's ability to perform feeding behaviours and the ability of the prey to respond to the strike. We argue that suction accuracy is an emergent property of all three factors and is an integrative measure of capture performance. Suction accuracy will decrease if the predator startles the prey during the approach, if the predator fails to generate peak forces at the correct time and position relative to the prey and if the prey responds correctly away from the predator. Therefore, to maintain accuracy and ensure success, predators must integrate approach and feeding behaviours to prevent or overcome prey responses. Although prey behaviour plays a large role in predator success [4,5,8] and preliminary data support the role of prey behaviour in determining predator success (unpublished data 2014), we were not able to address prey behaviour directly, so we focus our discussion on the role of predator behaviour.

Predators often modulate kinematics in response to prey type to increase the chance of success on evasive prey [56], and these changes are likely the mechanism for modulating the size and shape of the IVW. Predators attack evasive prey faster and from a greater distance [12,13,21,25,56] presumably to reduce the amount of time for prey to escape. Additionally, predators use a greater magnitude and rate of cranial expansion [57,58] leading to an increased magnitude of buccal pressure change [13,59] and therefore suction. Interestingly, although reduced time to peak gape (rate of expansion) increases peak fluid speed, and therefore suction force [17,28], it is not a strong predictor of suction volume [29]. This may be due to the interaction between timing and magnitude, where faster expansion results in less time to ingest particles, limiting any substantial influence on volume change.

We found that predators increased ram speed and gape size when capturing evasive prey, resulting in larger and more elongate ingested volumes in two of three predators (table 5; figure 6 and electronic supplementary material, figure S2). This modulation presumably increased the chance of predator success on evasive prey, but in *L. macrochirus* suction accuracy was low, and this modulation was not extensive enough to achieve the level of success observed in *M. salmoides*. This may be due to a small mouth size that limits the ability to capture larger prey. Alternatively, the large gape and high ram speed of *M. salmoides* is effective at capturing non-evasive prey at reduced magnitudes. Modulation was not observed in *L. cyanellus*, resulting in poor success. This species was not allowed to ambush prey from a hiding spot (as was common in holding tanks), which may be a more optimal strategy to prevent detection by prey and could explain similar IVW characteristics regardless of prey type. However, in general, the relationships between kinematics and suction volume provide the mechanism for changing the shape and size of the IVW when predators encounter evasive and non-evasive prey types, which represents a novel level of performance modulation.

Suction accuracy refers to the ability to correctly position and time the suction volume relative to the prey, and predators can control this accuracy in two ways: by modifying body orientation and position or by modifying the size and shape of the IVW. These two behaviours are not mutually exclusive, because forward movement increases the volume of particles ingested by suction [28,29]. We show how the size and shape of the IVW is modified with changes in peak gape height and ram speed at peak gape, and these variables represent the roles of feeding and locomotor performance in prey capture. Therefore, the ability to coordinate feeding and locomotor behaviours may be a key factor maximizing success. Surprisingly, most differences between species and prey types were in shape and size of the ingested volume rather than suction accuracy. Similar levels of accuracy observed across species may be achieved by compensating for feeding performance with approach strategies, or vice versa. Typically, feeding and locomotion are considered independent performance regimes, but during prey capture, the ability to integrate these behaviours in a way that results in timing and positioning the IVW correctly with respect to the prey may be critical for ensuring success.

### 4.3. Ecological relevance

Several studies have attempted to describe the ability of suction-feeding predators to correctly position and time their strikes on prey [6,8,10,29], but none have empirically tested the hypothesis that suction accuracy predicts success. Our work supports this hypothesis, and by establishing the link between suction accuracy and success we provide the ecological relevance of accuracy for suction-feeding predators, so that it can be used as a measure of prey capture performance [7]. Accuracy requires integration of locomotor and feeding behaviours, so that the suction volume is correctly positioned and timed

relative to the prey, and in this way, it represents a more holistic measure of performance than examining performance of either system in isolation [60], and adds insights into the prey capture strategies of predators.

Our study only examined the differences in three species of centrarchid predators, but the accessibility of suction accuracy as a measure of performance makes it possible to examine differences across a wider range of taxa. The next steps should be to determine whether the patterns observed in these species are also reflected in more generalized species such as those in the *Pomoxis* clade, or molluscivorous species specialized for prey processing, rather than capturing (e.g. *L. microlophus* or *L. gibbosus*). Additionally, patterns of accuracy and capture success should be examined in other non-Centrarchid taxa to validate the generality of our study. Our work suggests mechanisms by which ecological and evolutionary specialization affect the ability to capture prey, but to address this question empirically, macroevolutionary analyses of prey capture performance and success are necessary.

**Acknowledgements.** We thank Zach Zboch for assistance in collecting specimens and Kevin Dinh, Darryl Cheung, and Sofia Irribarren for assistance with digitizing. The following people provided assistance with Matlab code: Ty Hedrick, Jeff Olberding, Matt McHenry, Alexandra Birn-Jeffrey and Simon Wilshin. Matt McHenry, Dan Ozer, Kathleen Foster and Jeff Olberding provided helpful discussion on project design and interpretation. We thank four anonymous reviewers, Bill Stewart, Matt McHenry and Dan Ozer for helpful comments on earlier versions of the manuscript.

**Data accessibility.** Raw data, sample video, and sample smoothed points: Dryad doi:10.105061/dryad.hf591. Matlab code, sample smoothed points, PIV IVW coordinates (also available in raw data file): primary author's personal website. Supplemental methods, tables, and figures: journal supplement (note that this also contains information describing the locations and information contained in all supplemental material).

**Funding statement.** This work was supported by start-up funds to T.E.H. and a Sigma Xi grant in aid of research to E.A.K.

## References

- Shiffman E, Eilam D. 2004 Movement and direction of movement of a simulated prey affect the success rate in barn owl *Tyto alba* attack. *J. Avian Biol.* **35**, 111–116. (doi:10.1111/j.0908-8857.2004.03257.x)
- Combes SA, Salcedo MK, Pandit MM, Iwasaki JM. 2013 Capture success and efficiency of dragonflies pursuing different types of prey. *Integr. Comp. Biol.* **53**, 787–798. (doi:10.1093/icb/ict072)
- Britton AR, Jones G. 1999 Echolocation behaviour and prey-capture success in foraging bats: laboratory and field experiments on *Myotis daubentonii*. *J. Exp. Biol.* **202**, 1793–1801.
- Walker JA, Ghahambor CK, Griset OL, McKenney D, Reznick DN. 2005 Do faster starts increase the probability of evading predators? *Funct. Ecol.* **19**, 808–815. (doi:10.1111/j.1365-2435.2005.01033.x)
- Stewart WJ, Cardenas GS, McHenry MJ. 2013 Zebrafish larvae evade predators by sensing water flow. *J. Exp. Biol.* **216**, 388–398. (doi:10.1242/jeb.072751)
- Drost MR. 1987 Relation between aiming and catch success in larval fishes. *Can. J. Fish. Aquat. Sci.* **44**, 304–315. (doi:10.1139/f87-039)
- Irschick DJ, Meyers JJ, Husak JF, Le Galliard J. 2008 How does selection operate on whole-organism functional performance capacities? A review and synthesis. *Evol. Ecol. Res.* **10**, 177–196.
- Holzman R, Collar DC, Mehta RS, Wainwright PC. 2012 An integrative modeling approach to elucidate suction-feeding performance. *J. Exp. Biol.* **215**, 1–13. (doi:10.1242/jeb.057851)
- Maie T, Furtek S, Schoenfuss HL, Blob RW. 2014 Feeding performance of the Hawaiian sleeper, *Eleotris sandwicensis* (Gobioidae: Eleotridae): correlations between predatory functional modulation and selection pressures on prey. *Biol. J. Linn. Soc.* **111**, 359–374. (doi:10.1111/bij.12214)
- Nauwelaerts S, Wilga CD, Lauder GV, Sanford CP. 2008 Fluid dynamics of feeding behaviour in white-spotted bamboo sharks. *J. Exp. Biol.* **211**, 3095–3102. (doi:10.1242/jeb.019059)
- Lauder GV. 1985 Aquatic feeding in lower vertebrates. In *Functional vertebrate morphology* (eds M Hildebrand, DM Bramble, KF Liem, DB Wake), pp. 210–229. Cambridge, MA: Harvard University Press.
- Wainwright PC, Ferry-Graham LA, Waltzek TB, Carroll AM, Hulsey CD, Grubich JR. 2001 Evaluating the use of ram and suction during prey capture by cichlid fishes. *J. Exp. Biol.* **204**, 3039–3051.
- Norton SF, Brainerd EL. 1993 Convergence in the feeding mechanics of ecomorphologically similar species in the Centrarchidae and Cichlidae. *J. Exp. Biol.* **176**, 11–29.
- Alexander RM. 1967 *Functional design in fishes*. London, UK: Hutchinson University Library.
- Muller M, Osse JWM. 1984 Hydrodynamics of suction feeding in fish. *Trans. Zool. Soc. Lond.* **37**, 51–135. (doi:10.1111/j.1096-3642.1984.tb00068.x)
- Weihls D. 1980 Hydrodynamics of suction feeding of fish in motion. *J. Fish Biol.* **16**, 425–433. (doi:10.1111/j.1095-8649.1980.tb03720.x)
- Day SW, Higham TE, Cheer AY, Wainwright PC. 2005 Spatial and temporal patterns of water flow generated by suction-feeding bluegill sunfish *Lepomis macrochirus* resolved by particle image velocimetry. *J. Exp. Biol.* **208**, 2661–2671. (doi:10.1242/jeb.01708)
- Day SW, Higham TE, Wainwright PC. 2007 Time resolved measurements of the flow generated by

- suction feeding fish. *Exp. Fluids*. **43**, 713–724. (doi:10.1007/978-3-642-11633-9\_8)
19. Holzman R, Day SW, Wainwright PC. 2007 Timing is everything: coordination of strike kinematics affects the force exerted by suction feeding fish on attached prey. *J. Exp. Biol.* **210**, 3328–3336. (doi:10.1242/jeb.008292)
  20. Ferry-Graham LA, Wainwright PC, Lauder GV. 2003 Quantification of flow during suction feeding in bluegill sunfish. *Zoology* **106**, 159–168. (doi:10.1078/0944-2006-00110)
  21. Norton SF. 1991 Capture success and diet of cottid fishes: the role of predator morphology and attack kinematics. *Ecology* **72**, 1807–1819. (doi:10.2307/1940980)
  22. McLaughlin RL, Grant JWA, Noakes DLG. 2000 Living with failure: the prey capture success of young brook charr in streams. *Ecol. Freshw. Fish.* **9**, 81–89. (doi:10.1034/j.1600-0633.2000.90109.x)
  23. Rincón PA, Bastir M, Grossman GD. 2007 Form and performance: body shape and prey-capture success in four drift-feeding minnows. *Oecologia* **152**, 345–355. (doi:10.1007/s00442-006-0651-5)
  24. Coughlin DJ. 1994 Suction prey capture by clownfish larvae (*Amphiprion perideraion*). *Copeia* **1994**, 242–246. (doi:10.2307/1446695)
  25. Nyberg DW. 1971 Prey capture in the largemouth bass. *Am. Midl. Nat.* **86**, 128–144. (doi:10.2307/2423693)
  26. Webb PW, Skadsen JM. 1980 Strike tactics of *Esox*. *Can. J. Zool.* **58**, 1462–1469. (doi:10.1139/z80-201)
  27. Coughlin DJ. 1991 Ontogeny of feeding behavior of first-feeding Atlantic salmon (*Salmo salar*). *Can. J. Fish. Aquat. Sci.* **48**, 1896–1904. (doi:10.1139/f91-225)
  28. Higham TE, Day SW, Wainwright PC. 2005 Sucking while swimming: evaluating the effects of ram speed on suction generation in bluegill sunfish *Lepomis macrochirus* using digital particle image velocimetry. *J. Exp. Biol.* **208**, 2653–2660. (doi:10.1242/jeb.01682)
  29. Higham TE, Day SW, Wainwright PC. 2006 Multidimensional analysis of suction feeding performance in fishes: fluid speed, acceleration, strike accuracy and the ingested volume of water. *J. Exp. Biol.* **209**, 2713–2725. (doi:10.1242/jeb.02315)
  30. Van Leeuwen JL. 1984 A quantitative study of flow in prey capture by rainbow trout, *Salmo gairdneri* with general consideration of the actinopterygian feeding mechanism. *Trans. Zool. Soc. Lond.* **37**, 171–227. (doi:10.1111/j.1096-3642.1984.tb00070.x)
  31. Sanford CPJ, Wainwright PC. 2002 Use of sonomicrometry demonstrates the link between prey capture kinematics and suction pressure in largemouth bass. *J. Exp. Biol.* **205**, 3445–3457.
  32. Bishop KL, Wainwright PC, Holzman R. 2008 Anterior-to-posterior wave of buccal expansion in suction feeding fishes is critical for optimizing fluid flow velocity profile. *J. R. Soc. Interface* **5**, 1309–1316. (doi:10.1098/rsif.2008.0017)
  33. Holzman R, Day SW, Mehta RS, Wainwright PC. 2008 Jaw protrusion enhances forces exerted on prey by suction feeding fishes. *J. R. Soc. Interface* **5**, 1445–1457. (doi:10.1098/rsif.2008.0159)
  34. Carroll AM, Wainwright PC. 2009 Energetic limitations on suction feeding performance in centrarchid fishes. *J. Exp. Biol.* **212**, 3241–3251. (doi:10.1242/jeb.033092)
  35. Lauder GV. 1983 Functional and morphological bases of trophic specialization in sunfishes (Teleostei, Centrarchidae). *J. Morphol.* **178**, 1–21. (doi:10.1002/jmor.1051780102)
  36. Wainwright PC. 1996 Ecological explanation through functional morphology: the feeding biology of sunfishes. *Ecology* **77**, 1336–1343. (doi:10.2307/2265531)
  37. Wainwright PC, Shaw SS. 1999 Morphological basis of kinematic diversity in feeding sunfishes. *J. Exp. Biol.* **202**, 3101–3110.
  38. Collar DC, Near TJ, Wainwright PC. 2005 Comparative analysis of morphological diversity: does disparity accumulate at the same rate in two lineages of centrarchid fishes? *Evolution* **59**, 1783–1794. (doi:10.1111/j.0014-3820.2005.tb01826.x)
  39. Collar DC, Wainwright PC. 2006 Discordance between morphological and mechanical diversity in the feeding mechanism of centrarchid fishes. *Evolution* **60**, 2575–2584. (doi:10.1111/j.0014-3820.2006.tb01891.x)
  40. Wainwright PC. 2007 Functional versus morphological diversity in macroevolution. *Annu. Rev. Ecol. Evol. Syst.* **38**, 381–401. (doi:10.1146/annurev.ecolsys.38.091206.095706)
  41. Near TJ, Bolnick DI, Wainwright PC. 2005 Fossil calibrations and molecular divergence time estimates in centrarchid fishes (Teleostei: Centrarchidae). *Evolution* **59**, 1768–1782. (doi:10.1111/j.0014-3820.2005.tb01825.x)
  42. Collar DC, O'Meara BC, Wainwright PC, Near TJ. 2009 Piscivory limits diversification of feeding morphology in centrarchid fishes. *Evolution* **63**, 1557–1573. (doi:10.1111/j.1558-5646.2009.00626.x)
  43. Carroll AM, Wainwright PC, Huskey SH, Collar DC, Turingan RG. 2004 Morphology predicts suction feeding performance in centrarchid fishes. *J. Exp. Biol.* **207**, 3873–3881. (doi:10.1242/jeb.01227)
  44. Holzman R, Day SW, Mehta RS, Wainwright PC. 2008 Integrating the determinants of suction feeding performance in centrarchid fishes. *J. Exp. Biol.* **211**, 3296–3305. (doi:10.1242/jeb.020909)
  45. Burnham KP, Anderson DR. 2002 *Model selection and multimodal inference: a practical information-theoretic approach*, 2nd edn. New York, NY: Springer.
  46. Anderson DR. 2008 *Model based inference in the life sciences: a primer on evidence*. New York, NY: Springer.
  47. Hedrick TL. 2008 Software techniques for two- and three-dimensional kinematic measurements of biological and biomimetic systems. *Bioinspir. Biomim.* **3**, 034001. (doi:10.1088/1748-3182/3/3/034001)
  48. Riskin DK, Willis DJ, Iriarte-D J, Hedrick TL, Kostandov M, Chen J, Laidlaw DH, Breuer KS, Swartz SM. 2008 Quantifying the complexity of bat wing kinematics. *J. Theor. Biol.* **254**, 604–615. (doi:10.1016/j.jtbi.2008.06.011)
  49. Muller M, Osse JWM, Verhagen JHG. 1982 A quantitative hydrodynamic model of suction feeding in fish. *J. Theor. Biol.* **95**, 49–79. (doi:10.1016/0022-5193(82)90287-9)
  50. van Leeuwen JL, Muller M. 1984 Optimum sucking techniques for predatory fish. *Trans. Zool. Soc. Lond.* **37**, 137–169. (doi:10.1111/j.1096-3642.1984.tb00069.x)
  51. Camp A, Brainerd E. In press. Role of axial muscles in powering mouth expansion during suction feeding in largemouth bass. *J. Exp. Biol.* (doi:10.1242/jeb.095810)
  52. Hernandez LP. 2000 Intraspecific scaling of feeding mechanics in an ontogenetic series of zebrafish, *Danio rerio*. *J. Exp. Biol.* **203**, 3033–3043.
  53. Fuiman LA, Webb PW. 1988 Ontogeny of routine swimming activity and performance in zebra danios (Teleostei: Cyprinidae). *Anim. Behav.* **36**, 250–261. (doi:10.1016/S0003-3472(88)80268-9)
  54. Lauder GV, Shaffer HB. 1986 Functional design of the feeding mechanism in lower vertebrates: unidirectional and bidirectional flow systems in the tiger salamander. *Zool. J. Linn. Soc.* **88**, 277–290. (doi:10.1111/j.1096-3642.1986.tb01191.x)
  55. Miller BT, Larsen Jr JH. 1989 Feeding performance in aquatic postmetamorphic newts (Urodela: Salamandridae): are bidirectional flow systems necessarily inefficient? *Can. J. Zool.* **67**, 2414–2421. (doi:10.1139/z89-342)
  56. Nemeth DH. 1997 Modulation of attack behavior and its effect on feeding performance in a trophic generalist fish, *Hexagrammos decagrammus*. *J. Exp. Biol.* **200**, 2155–2164.
  57. Ferry-Graham LA, Wainwright PC, Westneat MW, Bellwood DR. 2001 Modulation of prey capture kinematics in the cheeklined wrasse *Oxycheilinus digrammus* (Teleostei: labridae). *J. Exp. Zool.* **290**, 88–100. (doi:10.1002/jez.1038)
  58. Van Wassenbergh S, De Rechter D. 2011 Piscivorous cyprinid fish modulates suction feeding kinematics to capture elusive prey. *Zoology* **114**, 46–52. (doi:10.1016/j.zool.2010.10.001)
  59. Nemeth DH. 1997 Modulation of buccal pressure during prey capture in *Hexagrammos decagrammus* (Teleostei: Hexagrammidae). *J. Exp. Biol.* **200**, 2145–2154.
  60. Kane EA, Higham TE. 2011 The integration of locomotion and prey capture in divergent cottid fishes: functional disparity despite morphological similarity. *J. Exp. Biol.* **214**, 1092–1099. (doi:10.1242/jeb.052068)